Asian Journal of Chemistry; Vol. 25, No. 2 (2013), 628-632

ASIAN JOURNAL OF CHEMISTRY

http://dx.doi.org/10.14233/ajchem.2013.11690

Effect of Reaction Time on Highly Ordered TiO_2 Nanotube Arrays Based Dye-Sensitized Solar Cells

SHANGHUA WANG[1,2], JINGBO ZHANG[1] and YUAN LIN[1,*]

[1]Beijing National Laboratory for Molecular Sciences, Key Laboratory of Photochemistry, Institute of Chemistry, Chinese Academy of Sciences, Beijing 100190, P.R. China
[2]Graduate School of Chinese Academy of Sciences, Beijing 100049, P.R. China

*Corresponding author: Fax: +86 10 82617315; Tel: +86 10 82615031; E-mail: linyuan@iccas.ac.cn

(*Received*: 6 February 2011; *Accepted*: 9 August 2012) AJC-11943

Highly ordered TiO_2 nanotube arrays (TNAs) were fabricated by anodizing titanium foils in F-containing electrolyte for different time. The crystalline and morphology of the prepared TiO_2 nanotube arrays were studied by X-ray diffraction patterns and scanning electron microscope. The influences of reaction time on the prepared TiO_2 nanotube arrays were carefully examined. The results showed that the surface area of TiO_2 nanotube arrays increased with reaction time, meanwhile resistance on photoanode/electrolyte interface decreased with reaction time. Too long reaction time will not increase the surface area of TiO_2 nanotube arrays. When the prepared TiO_2 nanotube arrays were used on dye-sensitized solar cells (DSSCs), a light to electricity conversion efficiency (η) of 5.95 % was obtained when illuminated on back side which is a high efficiency considering without further treatment of TiO_2 nanotube arrays.

Key Words: TiO_2 nanotube arrays, Dye-sensitized solar cells, Light to electricity conversion efficiency, Photoanode.

INTRODUCTION

Dye-sensitized solar cells is considered as a relatively low cost solar cell technology and a potential alternative to silicon solar cells since the original work of O'Regan and Grätzel[1]. Traditional photoanode of dye-sensitized solar cells is usually made by sintering a paste consisting of colloidal oxide particles with sizes in the 10^{-30} nm range. Since Grimes and co-workers[2] first reported the preparation of uniform TiO_2 nanotube arrays in 2001, much attention have been paid to TiO_2 nanotube arrays because of the inherent excellent properties of TiO_2 nanotube arrays[3-7]. Highly ordered TiO_2 nanotube arrays is a potential alternative to films fabricated by the sol-gel route because they combine high surface area with well-defined pore geometry[8-11]. The arrangement of the highly ordered TiO_2 nanotube arrays perpendicular to the surface permits facile charge transfer along the length of the nanotube, thereby reducing the losses incurred by charge-hopping across the nanoparticle grain boundaries[12].

The morphologies of TiO_2 nanotube arrays are determined by experimental conditions. The diameter, length and wall thickness varies due to experimental conditions[7,13-20]. In present work, we prepared TiO_2 nanotube arrays by anodizing titanium foils in F^- based electrolyte for different time and found 50 h prepared TiO_2 nanotube arrays based dye-sensitized solar cells have the highest light to electricity conversion efficiency. But when we increase the reaction time the surface area of TiO_2 nanotube arrays and the light to electricity conversion efficiency of TiO_2 nanotube arrays based dye-sensitized solar cells began to decrease.

EXPERIMENTAL

Lithium iodide, 4-*tert*-butylpyridine, 1-hexyl-2,3-dimethylimidazolium iodide, 3-methoxyacetonitrile and iodine were purchased from Acros. Ethylene glycol, acetone, methanol, ethanol, isopropanol, ammonium fluoride, acetonitrile, tetra-*n*-butyltitanate, butanol, acetic acid, NaOH and 2,4-diisocyanatotoluene (TDI) were purchased from Beijing Chemical Company (analytic reagent grade). Ti foils were purchased from Alfa Aesar.

Preparation of photoanode and counter electrode: Titanium foils (99.5 % in purity and 0.2 mm in thickness) with a size of 1 cm × 3 cm were polished with silicon carbide sand paper of 400, 600, 800, 1000 and 1500 grit in sequence, ultrasonically cleaned in acetone, isopropanol, methanol and finally rinsed with deionized water for 15 min. Then they were dried under a flowing N_2 stream and used instantly.

The cleaned titanium foils were electrochemical anodized in an electrolyte containing 0.5 wt % NH_4F, 1 wt % deionized water and 98.5 wt % ethylene glycol. Anodization was carried out in an electrochemical cell by using a direct current source

at a constant voltage of 60 V, with a platinum foil as counter electrode. The prepared TiO_2 nanotube arrays samples were annealed in air at 500 ºC for 2 h and then cooled to room temperature before being immersed overnight in a 0.3 mM ethanol solution of $Ru(dcbpy)_2(NCS)_2$ (N_3, Solaronix) for 24 h. The counter electrode was prepared as previously reported[21].

Cell assembly and dye desorption: The sensitized TiO_2 nanotube arrays were sandwiched together with transparent platinized counter electrodes fabricated from fluorine-doped tin oxide coated glass. The electrolyte, which contained 0.5 M 1-hexyl-2,3-dimethylimidazolium iodide, 0.05 M of iodine, 0.1 M of lithium iodide and 0.5 M of 4-*tert*-butylpyridine in 3-methoxyacetonitrile, was introduced into the space between the electrodes. The dye desorption was carried out in 5 mL 0.01 M NaOH to determine the dye loading on the surface of nanotubes.

Characterization and instruments: The morphologies of the annealed TiO_2 nanotube arrays were obtained on scanning electron microscope (S-4300 Hitachi). The crystal structures of the annealed and unannealed TiO_2 nanotube arrays were investigated using X-ray diffraction meter (Rigaku D/max-2500) using CuK_α radiation ($\lambda = 0.154$ nm) in the 2θ range of 0-80º. The concentrations of desorbed dye determined by UV-VIS spectroscopy (U-3010 Hitachi) were used to calculate the amount of dye loading on the surface of TiO_2 nanotube arrays. The DSSCs devices were operated with illumination on the back side and the photovoltaic data were recorded using a potentiostat/galvanostat (EG & G Princeton Applied Research, Model 273) under simulated AM1.5 irradiation (100 mW cm^{-2}). The active cell area was 0.2 cm^2. Electrochemical impedance spectra (EIS) were obtained by using Solartron 1255B frequency analyzer and Solartron SI 1287 electrochemical interface system.

RESULTS AND DISCUSSION

Characteristic of TiO_2 nanotube arrays: It is well recognized that the morphology of TiO_2 nanotube arrays prepared by anodization strongly depends on the electrochemical conditions. Fig. 1(a-c), (e) show the top views of the TiO_2 nanotube arrays anodic growth at 60 V for different reaction time (30, 40, 50 and 60 h). TiO_2 nanotube arrays are composed by highly ordered vertically oriented TiO_2 nanotubes which has an inner diameter of 90 nm and a wall thickness of 20 nm. It is evident that the neat and orderly surface tubular structures of TiO_2 nanotube arrays gradually destroyed with the reaction time increases. As shown in Fig. 1(a-b), the mouth of the nanotube is neat and orderly. When we increase the reaction time to 50 h, we found there some debris on the mouth of nanotube [Fig. 1(c)], these debris are ascribed to the dissolved part of nanotubes. Fig. 1(e) shows the mouth of the nanotube was dissolved and the surface of TiO_2 nanotube arrays becomes messy and disorderly. The cross-section images of TiO_2 nanotube arrays anodized for 50 and 60 h are shown in Fig. 1(d and f), when the reaction time was 50 h the TiO_2 nanotube arrays keeps its structure, but when the reaction time increased to 60 h the nanotube and the highly ordered structure was destroyed.

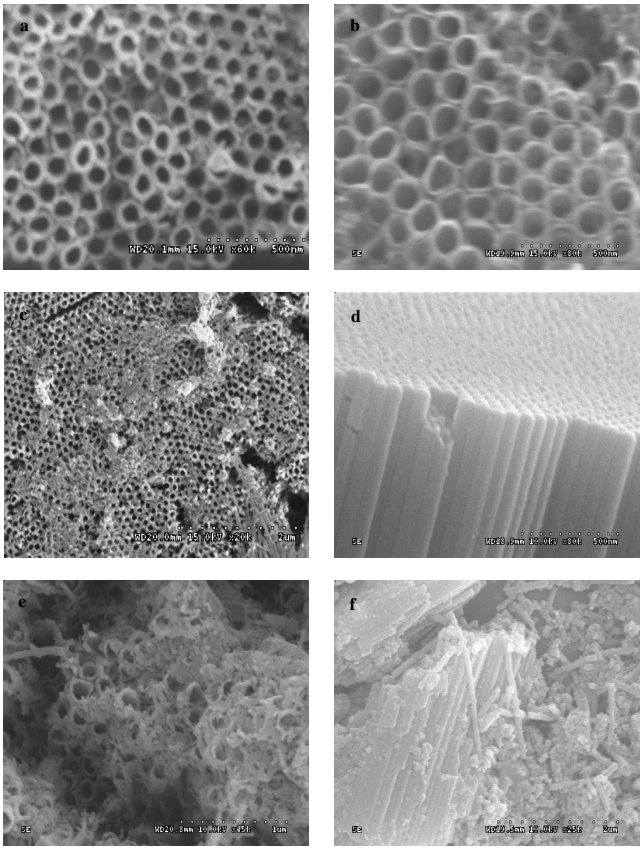

Fig. 1. SEM images of the prepared TiO_2 nanotube arrays. (a) Top view of 30 h prepared TiO_2 nanotube arrays; (b) Top view of 40 h prepared TiO_2 nanotube arrays; (c) Top view of 50 h prepared TiO_2 nanotube arrays; (d) Cross-section view of 50 h prepared TiO_2 nanotube arrays; (e) Top view of 60 h prepared TiO_2 nanotube arrays; (f) Cross-section view of 60 h prepared TiO_2 nanotube arrays

The anodization involved electrochemical oxidation of titanium into amorphous TiO_2 and chemical dissolution of the oxide into soluble titanium fluoride species (TiF_6^{2-}). The electrochemical and chemical reactions at the bottom and mouth of the nanotube are two main factors governing the growth of the nanotubes. At the bottom of the nanotube, the growth is governed by field-aided oxide growth, field-aided diffusion of ionic species and salvation at the oxide/electrolyte interface. The formation of TiO_2 nanotube arrays can be expressed as competition between electrochemical oxidation (reaction 1) and chemical dissolution (reaction 2):

$$Ti + 2H_2O = TiO_2 + 4H^+ + 4e^- \quad (1)$$

$$TiO_2 + 6F^- + 4H^+ = TiF_6^{2-} + 2H_2O \quad (2)$$

Metallic Ti is first oxidized to TiO_2 and then selectively dissolved by F^- ion. This makes the pore deeper and deeper. In reaction (1), $2H_2O = O_2 + 4H^+ + 4e^-$, so the dissolution of oxide layer occurring due to local acidity at the bottom of the TiO_2 nanotube leads to the progressive growth of nanotube length. For this, a proper acidic environment at the nanotube bottom is needed. While in the high viscosity electrolyte, water/glycerol, we can anodize Ti foils for longer time without destroy the structure of TiO_2 nanotube arrays and a steady tube growth is maintained. The reason for this drastic active/passive behaviour can be ascribed to the fact that OH^- in the bulk solution and H^+ produced *via* reaction process (reaction

1) have a lower diffusion rate in the viscous electrolyte. The pH value at the tube bottom is mainly controlled by the self-acidification process (reaction 1) and much less influenced by the bulk electrolyte pH value. As a result of the suitable viscosity of electrolyte, an acidic environment can be better controlled at the pore tip and this effect prevents dissolution at the pore tip. During the anodization process, the electrochemical oxide reaction rate at the bottom decreased gradually, but at the mouth the chemical dissolution reaction rate, which is mainly controlled by the bulk solution, remains unchanged. In the first stage of anodization process, the electrochemical oxide rate at the bottom is faster than the chemical dissolution rate. Therefore, the length of the tube increases with time. However, as time goes on, the electrochemical oxidation rate at the bottom becomes slower and slower, while the chemical dissolution rate at the mouth keeps constant, when the rates of the two reactions are the same, the length of nanotube stopped increasing. If further prolonging the reaction time, due to the rate of chemical dissolution at the mouth is greater than the rate of electrochemical oxidation, the mouth of the nanotube is dissolved, meanwhile at the interface metallic Ti/TiO_2 nanotube arrays the rate of formation of amorphous TiO_2 is slower than the chemical dissolution rate, so the TiO_2 nanotube arrays will be detached from the Ti substrate. The final outcome is the highly ordered structure of TiO_2 nanotube arrays was destroyed.

The dye loading amount is an important factor that affects the light to electricity conversion efficiency when the anodized TiO_2 nanotube arrays used as photoanode of dye-sensitized solar cells. The more dye molecules loading on the surface the larger short-circuit current density is obtained. Longer nanotube provides larger surface area for dye loading. Thus, the data of dye loading can be used for investigating the growth process of nanotube. The annealed TiO_2 nanotube arrays were immersed in 0.3 mM N3 ethanol solution overnight. After that the wall of the TiO_2 nanotube covered with a closely packed monolayer of N3 dye. The amount of dye loading (dl) can be determined from.

$$dl = \frac{AV}{\varepsilon S_0}$$

where A, V, ε and S_0 are the absorbance of the desorption solution, volume of desorption solution, molar extinction coefficient and geometric area of the photoanode, respectively. The data of dye loading were collected in Table-1. As shown in Table-1, the dye loading increased with the reaction time. This is ascribed to the rate of electrochemical oxide reaction at the bottom is faster than the chemical dissolution rate at the mouth and length of nanotube keeps increase, so more dye molecules loading on the surface of TiO_2 nanotube arrays. But the dye loading amount didn't increase when the reaction time was extended to 60 h. This is because in the extended time the rate of electrochemical oxide reaction at the bottom is slower than the chemical dissolution rate at the mouth and the mouth of the nanotube is dissolved, so the highly ordered structure of TiO_2 nanotube arrays was destroyed. For this, the dye loading amount decreased.

TABLE-1
DYE LOADING DATA AND PHOTOVOLTAIC PERFORMANCE PARAMETERS OF DSSCS

t (h)	dl (10^{-7} mol cm^{-2})	Jsc (mA cm^{-2})	Voc (mV)	ff	η (%)
10	0.50	6.72	756	0.74	3.74
20	0.65	7.84	726	0.74	4.21
30	0.94	7.57	742	0.75	4.24
40	1.06	8.33	722	0.71	4.28
50	1.44	10.35	748	0.77	5.95
60	1.34	10.30	716	0.64	4.74

t: reaction time. dl: dye loading amount. Jsc: short-circuit current density. Voc: open-circuit voltage. ff: fill factor. η: light to electricity conversion efficiency.

XRD analysis: Fig. 2 shows X-ray diffraction (XRD) patterns of the TiO_2 nanotube arrays before and after annealing. From the patterns it is evident that an amorphous phase is dominant before annealing (Fig. 2a). After annealing at 500 ºC for 2 h, the prepared TiO_2 nanotube arrays transferred from amorphous phase to polycrystalline anatase phase TiO_2 (Fig. 2b). The X-ray diffraction pattern of the annealed TiO_2 layer (Fig. 2b) shows several peaks at 25.3, 37.8, 48.0, 54.0, 55.0 and 62.7 º, inferring the crystallization and polycrystalline structure of the TiO_2 layer. According to their positions, the peaks are identified as the anatase phase of titanium oxide. The TiO_2 crystals exhibit a preferential orientation in a (101) facet, additionally the peaks (200), (103), (105) and (204) facets are also detected.

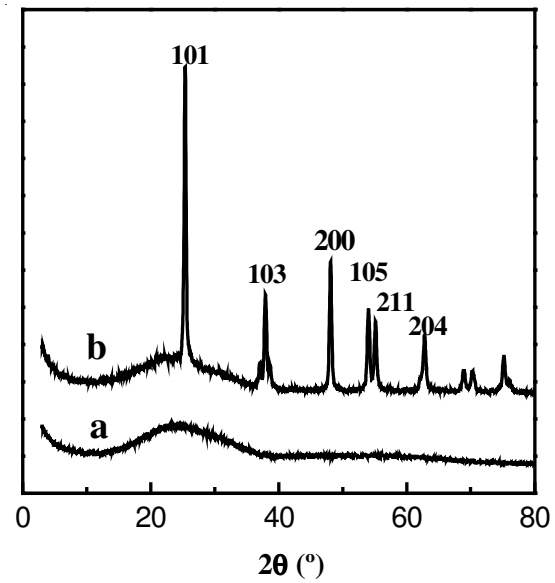

Fig. 2. XRD patterns of the TiO_2 nanotube arrays before (a) and after (b) sintering

Photovoltaic performances: The photovoltaic performance parameters of the TiO_2 nanotube arrays based dye-sensitized solar cells were collected in Table-1. We found 50 h prepared TiO_2 nanotube arrays based dye-sensitized solar cells have the highest η of 5.95 % and the trend of the η was consistent with the dye loading data. This is a high efficiency for the dye-sensitized solar cells based on TiO_2 nanotube arrays that without further treatment[11,21-23]. Meanwhile we found 60 h prepared TiO_2 nanotube arrays based dye-sensitized solar cells

have lower open-circuit voltage (Voc), short-circuit current density and fill factor. The lower short-circuit current density is due to the top tip of TiO_2 nanotube arrays was dissolved and the highly ordered structure was destroyed, so TiO_2 nanotube arrays can't provide as large surface area as the highly ordered, integrated TiO_2 nanotube arrays. The lower Voc is ascribed to the destroyed TiO_2 nanotube arrays provide more recombination center for electrons and increased the random diffusion path for electron. The disorder parameters of the TiO_2 nanotube arrays and integrated TiO_2 nanotube arrays were different significantly. The lower fill factor is probably ascribed to the charge transport in the destroyed TiO_2 nanotube arrays is not as efficient as in the integrated TiO_2 nanotube arrays. All these elements result in lower light to electricity conversion efficiency.

EIS analysis: Electrochemistry impedance spectroscopy was used to check the effect of reaction time on the interfacial charge transfer. The EIS were measured under 100 mW cm^{-2} illumination, using a perturbation of ± 10 mV over the open-circuit potential. The EIS are shown in Fig. 3a and the corresponding impedance data were collected in Table-2. The impedance spectrum of the dye-sensitized solar cells consists of two semicircles. The semicircle at high frequency is related to the charge-transfer process occurring at the Pt counter electrode/electrolyte interface and the one at low frequency is attributed to the charge-transfer process occurring at the photoanode/electrolyte interface. The insert is the equivalent circuit used for the fitting of impedance spectra for all dye-sensitized solar cells. Rs, Rct and Ri represent the series resistance, the charge-transfer resistance and the resistance in photoanode/electrolyte interface, respectively. The Rs indicated different reaction time prepared photoanodes have little effect on the series resistance. The slight differences in Rct were ascribed to the different counter electrodes used in our experiments. The Ri has the lowest value when the reaction time was 50 h. The larger resistance at the TiO_2 nanotube arrays/metallic Ti substrate interface when 60 h prepared TiO_2 nanotube arrays used in dye-sensitized solar cells probably due to less surface area for dye molecule anchoring and the destroyed structure of TiO_2 nanotube arrays limits the transmission of electronic and increases the resistance in photoanode/electrolyte interface. The lower Ri have positive effect in improving the short-circuit current density and finally improve the photo to electricity conversion efficiency. Additionally we studied the charge-transfer mechanism and the result was presented in Fig. 3b, the plot of the reciprocal of Ri *versus* dl has a good linearity. This means the nature of TiO_2 nanotube surface don't change as the growth of nanotube, the changes of Ri are caused by the changes in nanotube length.

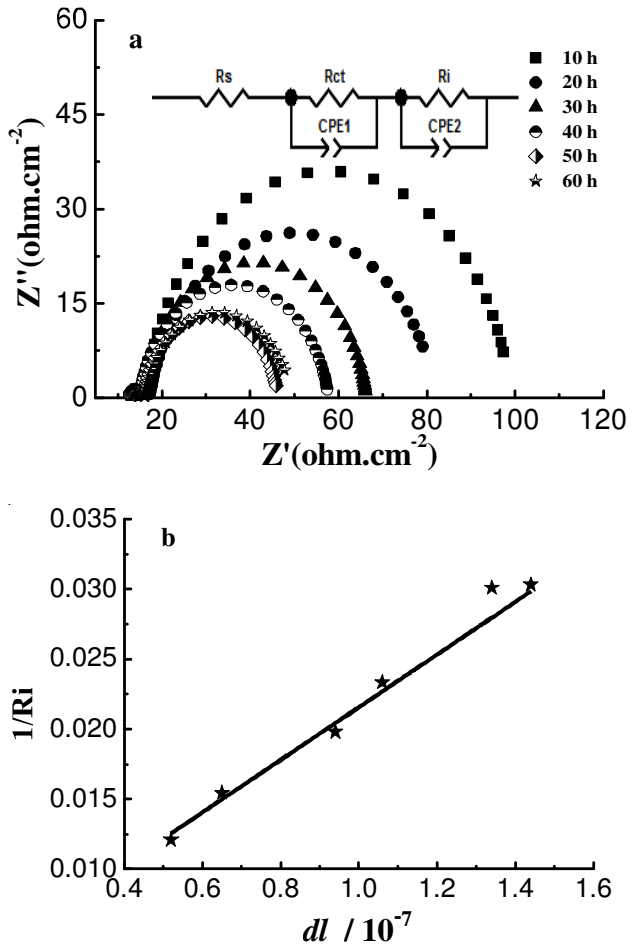

Fig. 3. (a) EIS plots of dye-sensitized solar cells based on different reaction time prepared TiO_2 nanotube arrays. (b) Plot of the reciprocal of Ri (the resistance in photoanode/electrolyte interface) *versus* dl (dye loading amount).

TABLE-2
PARAMETERS OF ELECTROCHEMISTRY IMPEDANCE SPECTROSCOPY OBTAINED FROM Fig. 3a

t (h)	Rs (Ω)	Rct (Ω)	Ri (Ω)
10	12.82	3.42	82.77
20	13.54	3.65	64.78
30	13.13	2.69	50.48
40	12.34	2.56	42.83
50	12.85	3.42	30.01
60	13.45	2.60	33.21

t: reaction time. Rs: series resistance. Rct: charge-transfer resistance in the Pt counter electrode/electrolyte interface. Ri: the resistance in photoanode/electrolyte interface.

Conclusion

In our study, we prepared highly ordered, surface smooth TiO_2 nanotube arrays. The XRD data showed after annealing the crystal style transferred from amorphous phase to polycrystalline anatase phase. The SEM images show that TiO_2 nanotube arrays has highly ordered architecture and the surface of TiO_2 nanotubes is smooth. The anodization time has three effects on the TiO_2 nanotube arrays: As anodization time increased the length of the TiO_2 nanotubes increased thereby increase the dye loading. Too long anodizaiton time will result will result in the top tip dissolution of TiO_2 nanotube arrays and the highly ordered structure was destroyed. And the Ri also increased due to the inefficient electron transportation and less surface area for dye molecules anchoring. The dye-sensitized solar cells showed a high efficiency of 5.95 % when 50 h prepared TiO_2 nanotube arrays used as photoanode. In order to get the excellent photoelectric performance for TiO_2 nanotube arrays based the dye-sensitized solar cells the appropriate experimental conditions are necessary for preparing TiO_2 nanotube arrays, which can keep the high orderly architecture of TiO_2 nanotube arrays and get large surface area.

ACKNOWLEDGEMENTS

This research is supported by the High-Tech Research and Development Program of China (2007AA05Z439), National Research Fund for Fundamental Key Project (2006CB202605), National Natural Science Foundation of China (20973183) and Foundation of Chinese academy of sciences (KJCX2-YW-386-2).

REFERENCES

1. B. O'Regan and M. Grätzel, *Nature*, **353**, 737 (1991).
2. D.W. Gong, C.A. Grimes, O.K. Varghese, W. Hu, R.S. Singh, Z.E. Chen and C. Dickey, *J. Mater. Res*., **16**, 3331 (2001).
3. Q. Zheng, B.X. Zhou, J. Bai, W.M. Cai and J.S. Liao, *Prog. Chem*., **19**, 117 (2007).
4. O.K. Varghese, D.W. Gong, M. Paulose, C.A. Grimes and E.C. Dickey, *J. Mater. Res*., **18**, 156 (2003).
5. H. Tsuchiya, J.M. Macak, L. Taveira, E. Balaur, A. Ghicov, K. Sirotna and P. Schmuki, *Electrochem. Commun*., **7**, 576 (2005).
6. J.M. Macak, H. Tsuchiya, L. Taveira, S. Aldabergerova and P. Schmuki, *Angew. Chem. Int. Ed*., **44**, 7463 (2005).
7. M. Paulose, H.E. Prakasam, O.K. Varghese, L. Peng, K.C. Popat, G.K. Mor, T.A. Desai and C.A. Grimes, *J. Phys. Chem. C*, **111**, 14992 (2007).
8. J.M. Macak, H. Tsuchiya, A. Ghicov and P. Schmuki, *Electrochem. Commun*., **7**, 1133 (2005).
9. G.K. Mor, K. Shankar, M. Paulose, O.K. Varghese and C.A. Grimes, *Nano Lett*., **6**, 215 (2006).
10. M. Paulose, K. Shankar, O.K. Varghese, G.K. Mor, B. Hardin and C.A. Grimes, *Nanotechnology*, **17**, 1446 (2006).
11. T. Stergiopoulos, A. Ghicov, V. Likodimos, D. S. Tsoukleris, J. Kunze, P. Schmuki and P. Falaras, *Nanotechnology*, **19**, 235602 (2008).
12. R. Tenne and C.N.R. Rao, *Philos. Trans. R. Soc. A*, **362**, 2099 (2004).
13. K. Shankar, G.K. Mor, H.E. Prakasam, S. Yoriya, M. Paulose, O.K. Varghese and C.A. Grimes, *Nanotechnology*, **18**, 065707 (2007).
14. J.B. Chen, C.W. Wang, B.H. Ma, Y. Li, J. Wang, R.Sh. Guo and W.M. Liu, *Thin Solid Films*, **517**, 4390 (2009).
15. J.L. Tao, J.L. Zhao, X.X. Wang, Y.R Kang and Y.X. Li, *Electrochem. Commun*., **10**, 1161 (2008).
16. W. Chanmanee, A. Watcharenwong, C.R. Chenthamarakshan, P.N. Kajitvichyanukul, R. de Tacconi and K. Rajeshwar, *J. Am. Chem. Soc*., **130**, 965 (2008).
17. Q.A. Nguyen, Y.V. Bhargava and T.M. Devine, *Electrochem. Commun*., **10**, 471 (2008).
18. J.H. Park, T.W. Leeb and M.G. Kang, *Chem. Commun*., **25**, 2867 (2008).
19. K. Shankar, J. Bandara, M. Paulose, H. Wietasch, O.K. Varghese, G.K. Mor, T.J. LaTempa, M. Thelakkat and C.A. Grimes, *Nano Lett*., **8**, 1654 (2008).
20. M. Paulose, H.E. Prakasam, O.K. Varghese, L. Peng, K.C. Popat, G.K. Mor, T.A. Desai and C.A. Grimes, *J. Phys. Chem. C*, **111**, 14992 (2007).
21. Y. Yang, X.H. Wang and L.T. Li, *J. Am. Ceram Soc*., **91**, 3086 (2008).
22. J.R. Jennings, A. Ghicov, L.M. Peter, P. Schmuki and A.B. Walker, *J. Am. Chem. Soc*., **130**, 13364 (2008).
23. D.J. Yang, H. Park, S.J. Cho, H.G. Kim and W.Y. Choi, *J. Phys. Chem. Solids*, **69**, 1272 (2008).